

Assessment of 2,4-dinitroanisole transformation using compound-specific isotope analysis after in situ chemical reduction of iron oxides

Matthew J. Berens[†], Thomas B. Hofstetter[‡], Jakov Bolotin[‡], and William A. Arnold^{,†}*

[†]Department of Civil, Environmental, and Geo- Engineering, University of Minnesota, 500
Pillsbury Drive SE, Minneapolis, MN, 55455-0116, United States

[‡]Eawag, Swiss Federal Institute of Aquatic Science and Technology, Department of
Environmental Chemistry, Überlandstrasse 133, CH-8600 Dübendorf and Institute of
Biogeochemistry and Pollutant Dynamics, ETH Zürich, CH-8092 Zürich, Switzerland

*Corresponding author: William A. Arnold; Phone: 612-625-8582; e-mail: arnol032@umn.edu

ABSTRACT

Ferrous iron-bearing minerals are important reductants in the contaminated subsurface but their availability for the reduction of anthropogenic pollutants is often limited by competition with other electron acceptors including microorganisms and poor Fe(II) accessibility in complex

hydrogeologic settings. The supply of external electron donors through *in situ* chemical reduction (ISCR) has been proposed as one remediation approach but the quantification of pollutant transformation is complicated by the perturbations introduced to the subsurface by ISCR. Here, we evaluate the application of compound specific isotope analysis (CSIA) for monitoring the reduction of 2,4-dinitroanisole (DNAN), a component of insensitive munitions formulations, by mineral-bound Fe(II) generated through ISCR of subsurface material from two field sites. Electron balances from laboratory experiments in batch and column reactors showed that 3.6% to 11% of the total Fe in the sediments was available for the reduction of DNAN and its partially reduced intermediates after dithionite treatment. The extent of DNAN reduction was successfully quantified from its N isotope fractionation measured in the column effluent based on the derivation of a N isotope enrichment factor, ϵ_N , derived from a comprehensive series of isotope fractionation experiments with numerous Fe(II)-bearing minerals as well as dithionite-reduced subsurface materials. Our observations illustrate the utility of CSIA as a robust analytical method to evaluate the success of *in situ* remediation through abiotic contaminant reduction.

INTRODUCTION

Ferrous iron (Fe(II)) associated with Fe-bearing minerals (e.g., iron (oxyhydr)oxides, clays, sulfide minerals) is an important reductant of many subsurface pollutants.¹⁻⁶ Despite an abundance of Fe(II) in the anoxic subsurface, pollutant reduction is often limited through competition with other potential electron acceptors and restricted pollutant transport and accessibility to reactive Fe(II)-bearing minerals in response to local hydrogeologic conditions. Several approaches have been evaluated to enhance the availability of reactive Fe(II) including biostimulation,^{7,8} bioaugmentation,^{9,10} additions of external electron donors (i.e., *in situ* chemical reduction; ISCR)

including dithionite,^{11,12} polysulfides,¹³ and (sulfidized) ZVI,^{14,15} and combinations thereof.¹⁶ To date, several of these strategies have been successfully applied to a number of environmental contaminants including heavy metals^{12,17,18} and chlorinated solvents.^{14,19,20}

One major challenge when applying an *in situ* (bio)remediation technique is providing a reliable evaluation of performance; it is difficult to quantify the amount of transformed contaminants from concentration measurements alone.^{21–23} For example, the need to (repeatedly) inject aqueous solutions containing electron donors into the subsurface introduces perturbations that may lead to pollutant dilution without degradation. Moreover, reduction of Fe(III) induces partial reductive dissolution and transformation of reactive Fe minerals and could mobilize solid-bound contaminants.^{17,24–26}

Compound specific isotope analysis (CSIA) is used to evaluate the extent of contaminant remediation by quantifying isotope enrichment of one or more elements in the residual pollutant.^{27–32} Because changes in stable isotope ratios (e.g., ¹⁵N/¹⁴N, ¹³C/¹²C) reflect reactions in which bond-cleavage occurs, isotope fractionation is minimally affected by non-degradative processes (e.g., sorption, dilution, phase transfer), thus circumventing many of the challenges associated with monitoring pollutant removal by concentration measurements alone.^{33,34} Despite the incorporation of CSIA into published monitored natural attenuation protocols, the majority of efforts have focused on biodegradation.^{21,27,28,35–37}

The recent emergence of 2,4-dinitroanisole (DNAN) in insensitive munitions formulations has caused concern because of its potential to contaminate large areas of land and water.^{38,39} We previously provided the first assessment of C and N isotope fractionation during abiotic DNAN reduction⁴⁰ but did not consider reductants beyond synthetic Fe-minerals. The Fe(II)-mediated reduction of DNAN generated isotope fractionation patterns that were indicative of certain reaction

pathways yet independent of DNAN reaction rates and solution chemistry (e.g., organic matter).⁴⁰ Given the heterogeneity of natural soils and sediments and the crystallographic diversity of Fe-minerals, however, it remains to be understood if DNAN isotope fractionation during reduction by Fe(II) of natural minerals deviates from that observed with synthetic analogs. Because multiple amendments of a given reductant are often required to achieve remediation targets with ISCR,^{12,41,42} it is similarly unknown how multiple redox cycles will affect the interpretation of CSIA results. Our findings suggest that because DNAN reduction by mineral-associated Fe(II) follows a common reaction pathway (i.e., abiotic nitro-group reduction^{28,35,40,43-45}), the associated isotope fractionation will not be affected despite the use of synthetic minerals or naturally collected ferruginous soils and sediments. This understanding could allow for DNAN to be a surrogate for other nitroaromatic compounds (NACs) including 2,4,6-trinitrotoluene (TNT) and analogs of nitrobenzene in the subsurface⁴⁶ and is important given the continuing need for *in situ* remediation techniques.⁴⁷ Numerous studies have indeed reported similar isotope enrichment factors from the abiotic reduction of several NACs in a range of experimental laboratory systems.⁴³⁻⁴⁵

In this study, we explored the application of CSIA for monitoring DNAN reduction during dithionite-based ISCR schemes. Sodium dithionite ($\text{Na}_2\text{S}_2\text{O}_4$) was chosen as the reductant because of its previous success for pollutant remediation in contaminated aquifers.^{11,19,41,48} We tested the reactivity of several Fe-bearing minerals and Fe-mineral containing sediments to promote DNAN reduction in batch reactors receiving amendments of aqueous Fe(II) and those receiving ISCR and used the distributions of reaction products to track the number of reduction equivalents transferred. The N and C isotope fractionation was measured during batch experiments to determine the bulk isotope enrichment factors (ϵ_N and ϵ_C) and apparent kinetic isotope effects (^{15}N -AKIE and ^{13}C -AKIE) associated with DNAN reduction. To simulate reducing environmental conditions,

subsurface materials collected from two field sites were exposed to DNAN following ISCR in continuous-flow column reactors. A modified Rayleigh fractionation equation was used to make quantitative estimates of DNAN degradation from N isotope ratios ($\delta^{15}\text{N}$) measured during each experiment. The accuracy of this approach was evaluated by conducting statistical comparisons of predicted versus observed DNAN degradation.

MATERIALS AND METHODS

A complete list of chemicals used in this study is provided in the Supporting Information (SI).

Laboratory conditions. All syntheses and batch experiments were performed in an anaerobic chamber (Coy Laboratory Products Inc.) with a 95% N_2 /5% H_2 atmosphere. Column experiments were performed in a NexGen anaerobic glovebox (Vacuum Atmospheres Company) maintained at <1 ppm O_2 with N_2 balance. Ultrapure water ($\geq 18.2 \text{ M}\Omega\cdot\text{cm}$) was generated by a Milli-Q Academic system (MilliporeSigma) and used to prepare all aqueous solutions. The ultrapure water was purged with N_2 gas (99.99%, Matheson) for at least 2 h prior to transfer into the chamber. Methanolic stock solutions were similarly prepared in deoxygenated methanol (ACS grade, MilliporeSigma). Laboratory equipment and reagents were evacuated in the exchange chamber and equilibrated overnight in the glovebag before use.

Material preparation and characterization. Subsurface materials were collected from the Twin Cities Army Ammunition Plant (TCAAP; Arden Hills, MN) and the Tinker Air Force Base (Tinker AFB; Oklahoma City, OK). Both sites have a history of contamination by organic pollutants and have required remediation efforts.^{1,49} Aquifer material from TCAAP was collected from the saturated zone by sonic drilling to a depth of 41–45 m. The material was dried, purged with N_2 gas, and stored inside the anaerobic chamber. Shallow sediment collected from Tinker

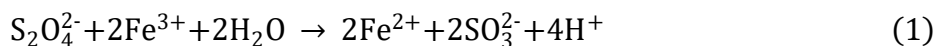
AFB was dried at 100 °C and stored in an amber jar under laboratory atmosphere. Both TCAAP and Tinker AFB materials were sieved by particle size to 350–425 µm before use. Synthetic magnetite nanoparticles were obtained from our previous work⁴⁰ and a suspension of rhombohedral hematite in deoxygenated, ultrapure water (~15 g/mL) was acquired from Voelz et al.⁵⁰

Each material was characterized by X-ray diffraction (XRD; Figure S1) to evaluate the purity (synthetic minerals) and bulk mineralogy (natural materials). No additional peaks were detected in patterns collected from synthetic minerals. The primary Fe-bearing phase as detectable by XRD in natural materials was magnetite (Fe₃O₄; TCAAP)^{1,51} and hematite (Fe₂O₃; Tinker AFB). Quartz (SiO₂; PDF #46-1045) was detected in each collected material as expected for highly weathered systems.

The total iron content (Fe_T) of TCAAP and Tinker AFB materials was quantified by inductively coupled plasma optical emission spectroscopy (ICP-OES). The ratio of Fe(II)/Fe(III) was estimated by acid dissolution in 3 M HCl^{52,53} and quantification by the ferrozine method⁵⁴ (Section S3). The amount of ion-exchangeable Fe(II) was estimated by saturating each material in 1 M CaCl₂ for 7 d and was below the limit of quantification in all samples (data not shown).⁵⁵ The magnetic portion of the TCAAP sediment (hereafter termed “TCAAP extract”) was separated from the bulk material with a neodymium magnet as described by Strehlau et al.⁵¹ and characterized by the same analyses. A summary of the relevant chemical and physical properties of all materials is provided in Table S1. Additional characterizations of hematite⁵⁰ and magnetite⁵¹ are reported elsewhere.

***In situ* chemical reduction.** For batch experiments receiving ISCR treatment, Fe-bearing materials were suspended in a solution of K₂CO₃/S₂O₄²⁻ (2:1 mol/mol) and rotated for 24 h, at

which point the suspension was separated via centrifugation and the supernatant discarded. The dithionite concentrations were selected so that enough dithionite was added to theoretically reduce one-tenth of the total Fe present (i.e., 1 mol $\text{S}_2\text{O}_4^{2-}$:20 mol Fe_T ; see eq 1). The $\text{K}_2\text{CO}_3/\text{S}_2\text{O}_4^{2-}$ ratio was chosen to buffer the 4 moles of H^+ released per 1 mole of dithionite consumed during iron reduction (eq 1).



The treated materials were then washed three times with carbonate buffer (10 mM, pH 7) by centrifugation to remove excess dithionite and its reaction products (e.g., sulfate, sulfite, thiosulfate),¹¹ suspended in carbonate buffer, and immediately used for DNAN reduction experiments in batch reactors. The Fe(II) content of each reduced material after ISCR was determined by acid dissolution as described above.

For column experiments, the materials were conditioned before adding dithionite by passing carbonate buffer (10 mM, pH 7.0) upwards through the column at 0.5 mL/min for 5 pore volumes. An aqueous solution of 1.25 mM sodium dithionite and 2.50 mM K_2CO_3 (pH 8–9) was then fed upward to the column at 0.25 mL/min for ~18–20 h. The low flow rate and long run (~30 pore volumes) time were used to allow enough time for the reaction to occur. Columns were flushed with ~10 pore volumes of carbonate buffer to remove unreacted dithionite and any oxidized sulfur species. The exact amount of pore volumes were chosen so that the same total amount of dithionite:Fe was introduced to each system (see eq 1). The total amount of iron in each column was in 20-fold excess to the dithionite added (i.e., 1 mol $\text{S}_2\text{O}_4^{2-}$:20 mol Fe_T) to target a reduction of one-tenth of Fe_T . Anoxic dithionite-buffer solutions were prepared fresh before each experiment to avoid loss of dithionite by aqueous disproportion; the rate of dithionite loss by aqueous disproportionation, however, has shown to be slower than Fe(III) reduction by dithionite.¹⁹

Batch experiments. Batch reactors were prepared in 35 mL borosilicate serum bottles according to previously described procedures.⁴⁰ First, a suspension of an untreated or dithionite-reduced Fe-bearing mineral in 10 mM carbonate buffer (pH 7.0) was added to each reactor. Solid loadings were varied from 1.0 g/L (hematite) to 143 g/L (TCAAP) such that DNAN transformation occurred in a similar time period. Aqueous Fe(II) was added to a concentration of 1 mM in reactors containing untreated materials. The dithionite-reduced materials did not receive amendments of Fe(II). Reactors were equilibrated for 21–24 h on an end-over-end rotator (Glas-col) at 40 rpm at which point the pH and aqueous Fe(II) concentration (via the Ferrozine assay,⁵⁴ Section S3) were measured. If necessary, the pH was adjusted back to 7.0 with 1 M HCl or 1 M NaOH and the aqueous Fe(II) content was restored to 1 mM in the reactors to which Fe(II) was added. Reactions were initiated by spiking DNAN from a methanolic stock solution to an initial concentration of 200 μ M. Reactors were placed on the rotator (40 rpm) and sacrificed at appropriate time points for concentration and stable isotope analyses. The pH (all reactors) and Fe(II) concentrations (Fe(II) amended reactors only) were closely monitored during reactions and maintained at 7.0 and 1 mM, respectively. Reactions were quenched by filtration through a 0.2 μ m nylon syringe filter (Chrom Tech) and stabilized with 1 M HCl (trace metals grade, MilliporeSigma) to pH<4 to prevent iron precipitation; DNAN did not react with aqueous Fe(II) under these conditions (data not shown). A portion (~1 mL) of each sample was analyzed for DNAN and intermediate/product concentrations by high pressure liquid chromatography (HPLC; method in SI) and the remaining sample (~18 mL) was stored at 4 °C for CSIA of DNAN.

The quantity of reduction equivalents transferred to DNAN from each reduced material was calculated with the assumption that 6 moles of electrons are required to reduce one nitro-moiety to the corresponding amine (see Scheme S1). The reduced products typically generated during

abiotic DNAN reduction are 2-amino-4-nitroanisole (2-ANAN), 4-amino-2-nitroanisole (4-ANAN), and 2,4-diaminoanisole (DAAN). Thus, 6 and 12 electrons are required for each mole of 2/4-ANAN and DAAN formed during DNAN reduction, respectively (Section S4 and eq S1).

Reactions in sediment columns. Borosilicate glass columns (Kimble FLEX-COLUMNS®; 2.5 cm I.D., 10 cm length) were packed with each natural material to uniform bulk ($\rho_b = 1.66 \pm 0.04$ g/cm³) and particle densities ($\rho_p = 2.68 \pm 0.05$ g/cm³). The mean porosity of sediment columns was 0.44 ± 0.05 (see Table S2). A flow adapter (Kimble) with fluorinated ethylene propylene (FEP) tubing was secured to the column inlet to prevent sediment migration and facilitate accurate bed height calculations. A polypropylene end cap was fixed at the column outlet. All feed solutions were amended with 10 mM NaCl to prevent the precipitation of insoluble species which may cause changes to flow characteristics. Pore volume and porosity were determined by saturating with 10 mM NaCl and a step input conservative tracer (100 mM NaBr) was used to characterize column flow and estimate the dispersion coefficient (Table S2; fitting details in SI). Bromide concentrations at the column outlet were measured with a conductivity probe (Oakton). Dispersion coefficients prior to experiments were 2.38 ± 0.24 and 2.53 ± 0.12 cm² s⁻¹ for TCAAP and Tinker AFB columns, respectively. All column materials were then reduced by sodium dithionite before experiments using DNAN.

Columns were equilibrated prior to DNAN reduction experiments by upward flow (0.5 mL/min) with 10 mM, pH 7.0 carbonate buffer including 10 mM NaCl for 5 pore volumes. Reactions were initiated by adding DNAN (200 μ M) to the feed solution and collecting effluent samples with an automated fraction collector (Bio-Rad Laboratories Inc). Experiments were terminated once the effluent concentration was equal to that of the feed solution. Columns were then flushed with carbonate buffer for several pore volumes to remove residual DNAN and any reaction products.

The column materials were then reduced again by sodium dithionite according to the method described above before further experiments using DNAN. The total number of reduction equivalents transferred to DNAN were calculated by integrating the concentrations of 2/4-ANAN and DAAN measured in the effluent (eq S2).

Compound specific isotope analysis. $^{13}\text{C}/^{12}\text{C}$ and $^{15}\text{N}/^{14}\text{N}$ isotope ratios of DNAN were measured following previously established procedures for gas chromatography / isotope ratio mass spectrometry (GC/IRMS) and solid phase micro extraction (SPME arrow) and are detailed in the Supporting Information.^{40,56-59} Isotope signatures were calculated from isotope ratios according to eq S4 relative to Vienna PeeDee Belemnite ($\delta^{13}\text{C}_{\text{VPDB}}$) and air ($\delta^{15}\text{N}_{\text{air}}$) reference standards.⁶⁰ Carbon and nitrogen isotope enrichment factors (ϵ_{C} , ϵ_{N}) were calculated by non-linear regression of C and N isotope signatures ($\delta^{13}\text{C}$, $\delta^{15}\text{N}$) vs the fraction of remaining substrate (c/c_0) as shown in eq 2.⁵⁹

$$\frac{\delta^{\text{hE}+1}}{\delta^{\text{hE}_0+1}} = \left(\frac{c}{c_0}\right)^{\epsilon_{\text{E}}} \quad (2)$$

where δ^{hE_0} is the initial isotope ratios of DNAN ($\delta^{13}\text{C}_0 = -37.4 \pm 0.1\%$, $\delta^{15}\text{N}_0 = -2.4 \pm 0.1\%$) as evaluated by elemental analysis (EA)/IRMS. Apparent kinetic isotope effects (^{13}C -AKIE, ^{15}N -AKIE) were determined from eq 3 based on the methods outlined by Elsner et al.⁶¹

$$^{\text{hE}}\text{-AKIE} = \frac{1}{1+n*\epsilon_{\text{E}}} \quad (3)$$

where n is a correction for isotopic dilution (n = 2 for primary ^{15}N -AKIEs and n = 1 for secondary ^{13}C -AKIEs). A linear regression of N and C isotope signatures was used to evaluate two-dimensional isotope fractionation trends. The slope of this regression ($\Lambda^{\text{N/C}}$) was calculated using eq S5 and is approximately equal to the ratio of the bulk isotope enrichment factors ($\epsilon_{\text{N}}/\epsilon_{\text{C}}$).

To estimate the extent of DNAN transformation during column experiments, measurements of $\delta^{15}\text{N}$ at the breakthrough front were applied to a modified form of the Rayleigh fractionation

equation (eq 4)²⁷ using an ϵ_N that was calculated based on the results of multiple datasets. This combined ϵ_N value (ϵ_N^*) was obtained by plotting all $\delta^{15}\text{N}$ measurements ($n = 122$) from batch experiments of DNAN reduction in this study and in Berens et al.⁴⁰ and performing a non-linear regression of the combined data according to eq 2. The extent of DNAN reduction was calculated with eq 4 from the deviation of measured $\delta^{15}\text{N}$ values from $\delta^{15}\text{N}_0$. using the combined ϵ_N^* value. We evaluated the accuracy of our estimates by performing a linear regression of the predicted vs measured values of c/c_0 and calculating the mean absolute error (MAE) of the predictions (eq 5).

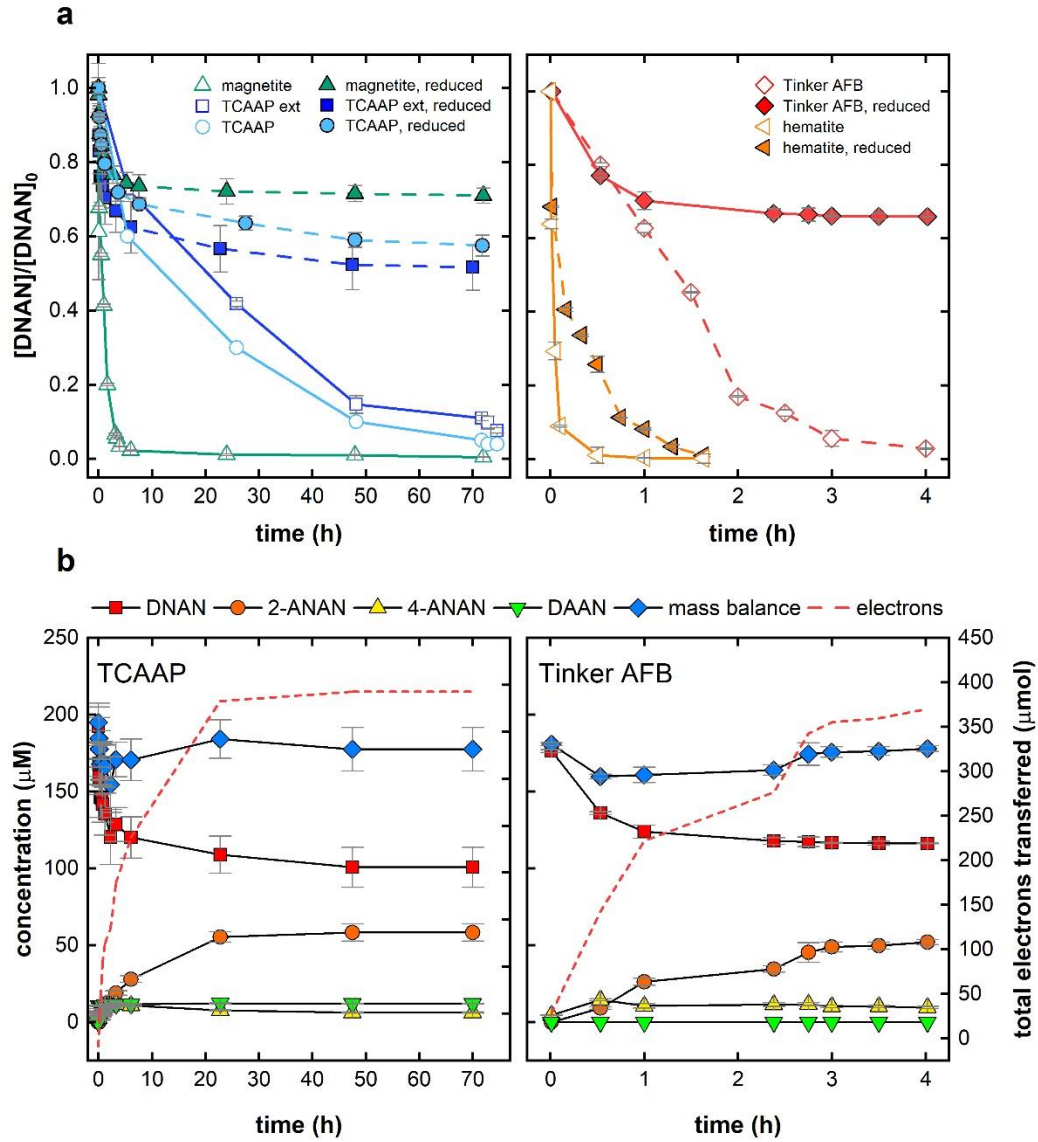
$$\frac{c}{c_0} = \left(\frac{\delta^{15}\text{N} + 1}{\delta^{15}\text{N}_0 + 1} \right)^{1/\epsilon_N^*} \quad (4)$$

$$\text{MAE} = \frac{\sum_{i=1}^n \left| (c/c_{0, \text{measured}})_i - (c/c_{0, \text{predicted}})_i \right|}{n} \quad (5)$$

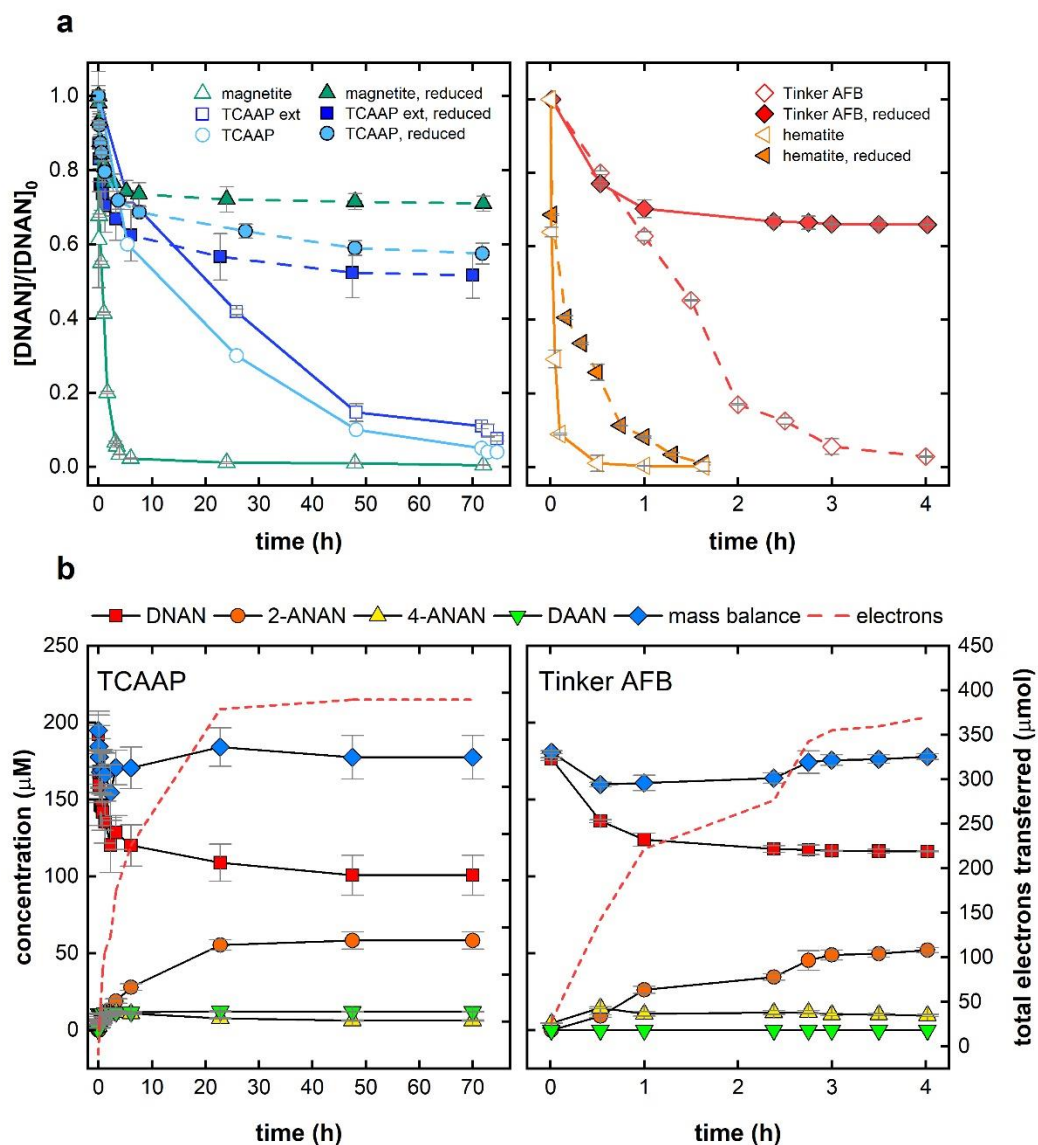
RESULTS AND DISCUSSION

Kinetic studies in batch reactors. Reduction of DNAN occurred in all reactors receiving

amendments of aqueous Fe(II) (



Figurea, open symbols) or ISCR by sodium dithionite (



Figurea, closed symbols). DNAN reduction was not observed in reactors containing only untreated minerals or aqueous Fe(II) alone (Figure S2). This supports the current understanding that Fe(II)-surface associations are required to mediate contaminant,^{2,62-66} and in particular DNAN,⁴⁰ reduction. The transformation products detected during DNAN reduction were 2-ANAN, 4-ANAN, and DAAN (Figure 1b). X-ray diffraction (XRD) patterns collected before and after ISCR showed no detectable changes in mineral composition following the treatments (Figure

S1) which suggests that the primary effect of ISCR on the structures of hematite and magnetite was the generation of surface-associated Fe(II) from oxide-Fe(III).

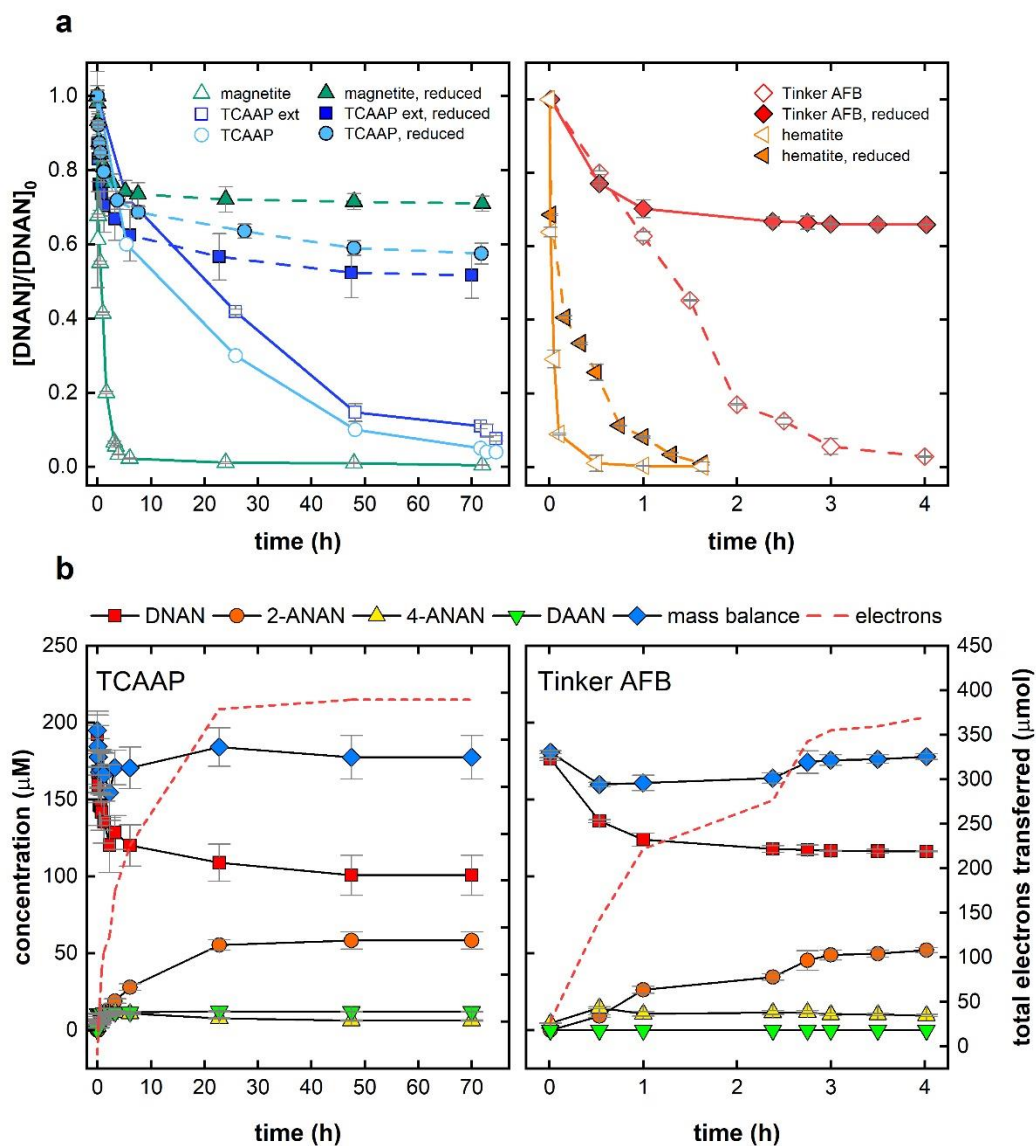


Figure 1. (a) Concentrations of DNAN during abiotic reduction by natural (TCAAP and Tinker AFB) and synthetic Fe-bearing (magnetite and hematite) materials. Experiments were performed with either untreated materials in the presence of 1 mM aqueous Fe(II) (open symbols) or with dithionite-reduced materials without additional Fe(II) (closed symbols). (b) Concentrations of DNAN, 2-ANAN, 4-ANAN, DAAN, and the cumulative number of electrons transferred during DNAN reduction by reduced TCAAP (left) and Tinker AFB (right) materials. All error bars represent standard deviations of triplicate reactors. Note the difference in time scales.

When aqueous Fe(II) was maintained (1 mM) throughout the batch experiments, all of the added DNAN was reduced to 2/4-ANAN or subsequently DAAN by each of the untreated minerals (Figure 1a, open symbols). In reactors receiving ISCR, only a portion of the DNAN was removed (Figure 1a, closed symbols), likely because of a limited supply of available electron equivalents (i.e., mineral-associated Fe(II)) generated during ISCR. To understand the extent of DNAN reduction in systems receiving ISCR, an electron balance was computed for each set of reactions (Figure 1b, dashed line). Accounting for the number of electrons transferred to DNAN as a function of the mineral-associated Fe(II) (i.e., mol e^- /mol Fe(II)) allowed for an evaluation of the efficiency of ISCR to generate reactive Fe(II).

Dithionite-reduced magnetite, TCAAP extract, and hematite promoted DNAN reduction with extents of electron transfer ranging from 0.359–0.603 mol e^- /mol Fe(II) (Table 1). These results suggest that not all available iron (Fe_T) was reduced to reaction-accessible Fe(II)⁶⁷ during ISCR. The washing of materials following dithionite treatments may have caused the release of Fe(II) that was not retained on mineral surfaces. It is also possible that potentially reducible oxide-Fe(III) was inaccessible to dithionite.^{68–71}

The lower standard reduction potential (E_H^0) of hematite (+0.793 V) versus magnetite (+1.053 V)⁷² may further explain the difference in electron transfer between the two systems. The reactivity of Fe-bearing minerals for pollutant reduction increases with lower E_H values as evidenced by hematite experiments. Moreover, magnetite stoichiometry ($x = Fe(II)/Fe(III)$) directly correlates with its intrinsic E_H values⁷³ and reactivity towards NAC reduction.⁷⁴ The magnetite used in this study ranged from partially oxidized ($x = 0.1$, TCAAP extract) to fully reduced, stoichiometric ($x = 0.5$, synthetic magnetite) materials. Low stoichiometry magnetite is a better oxidant and was thus more easily reduced by dithionite than the high stoichiometry magnetite (Table S1). These

results emphasize the potential benefits of ISCR to magnetite-bearing soils and sediments in which partially oxidized magnetite is common and may be amenable to ISCR leading to more stoichiometric and thus reactive magnetite.^{75,76}

Table 1. Total iron (Fe_T) and Fe(II) content of materials after dithionite treatments, and the cumulative number electrons transferred during DNAN reduction experiments.

system	Fe _T (μmol)	Fe(II) (μmol) ^c	total e ⁻ transferred (μmol) ^{d,e}	mol e ⁻ /mol Fe(II) ^e
<i>batch</i>				
TCAAP	3430 ^a	170	393 ± 1	2.31 ± 0.01
TCAAP extract	865 ^a	432	232 ± 1	0.536 ± 0.003
magnetite	903 ^b	451	162 ± 0.3	0.359 ± 0.001
Tinker AFB	2180 ^a	79.1	370 ± 0.4	4.68 ± 0.01
hematite	439 ^b	219	132 ± 1	0.603 ± 0.006
<i>column</i>				
TCAAP	25800 ^a	1280	183 ± 30	0.143 ± 0.022
Tinker AFB	17000 ^a	616	109 ± 10	0.176 ± 0.020

^aDetermined by ICP-OES. ^bCalculated from structural formulas of pure minerals. ^cCalculated by acid dissolution and quantification by the ferrozine method.⁵⁴ ^dCalculated using eqs S1–2. ^eUncertainties represent standard deviations of triplicate reactors.

The number of reduction equivalents transferred to DNAN from dithionite-reduced TCAAP (2.31 ± 0.01 mol e⁻/mol Fe(II)) and Tinker AFB (4.68 ± 0.01 mol e⁻/mol Fe(II)) materials exceeded the initial amount of Fe(II) present after dithionite treatments (Table 1). Despite targeted dithionite dosages to reduce one-tenth of the Fe_T, the calculated reduction efficiencies (i.e., Fe(II)/Fe_T from data in Table 1) of TCAAP and Tinker AFB materials during ISCR were only 4.95% and 3.62%, respectively. The low reduction efficiencies suggest that other reducible moieties were present in the natural materials which were reduced by dithionite and subsequently provided reducing equivalents for DNAN reduction.^{77,78} For example, the reversible transfer of electrons in the environment is often mediated by natural organic matter and humic substances, specifically those containing quinone moieties^{79–82}, and the TCAAP and Tinker materials contained 0.46% (w/w)

and 0.88% (w/w) organic matter, respectively. The electron-carrying capacity of these species plays a key role in both the reduction of substituted nitrobenzenes⁸³ and ferric iron.⁸⁴ Another possibility is that acid digestion of the materials to determine Fe(II) was incomplete. This is especially likely in materials with high Si content, such as phyllosilicates, because the Fe(III) is easily reduced by dithionite but Fe(II) extraction requires a rigorous treatment with H₂SO₄ and HF.^{67,85,86} This fraction of Fe(II) is a known strong reductant of NACs.^{3,87} The prominence of SiO₂ (Figure S1) and low Fe_T content of TCAAP and Tinker AFB materials (Table S1) suggests that a large share of Fe_T was associated with silicates.

Reactions in packed columns. To probe for the availability of reduction equivalents in flow-through systems, DNAN (200 μM) was introduced to column reactors containing dithionite-reduced TCAAP or Tinker AFB materials for five cycles of Fe(III) reduction by dithionite followed by DNAN exposure (Figure 2a-b). As shown in Figures 2c-d, ISCR in column reactors generated reaction-accessible electron equivalents in natural materials and promoted the reductive transformation of DNAN with a similar product distribution to the batch experiments (Figures 1c-d, Figure S3). It should be noted that DAAN concentrations exceeded the input DNAN concentration (up to 150%) during the early stages of experiments. To assess this phenomenon, the cumulative amount of DAAN measured in the column effluent was compared to the total amount of DNAN introduced. We found that the amount of DAAN in the peaks did not exceed the total amount of DNAN introduced to the columns. This indicated that DAAN was either associated with or retained on mineral surfaces and was then displaced by another solute, namely DNAN or 2/4-ANAN. The initial rapid production of DAAN leading to high concentration may have driven this interaction, and as aqueous concentrations dropped, other components in

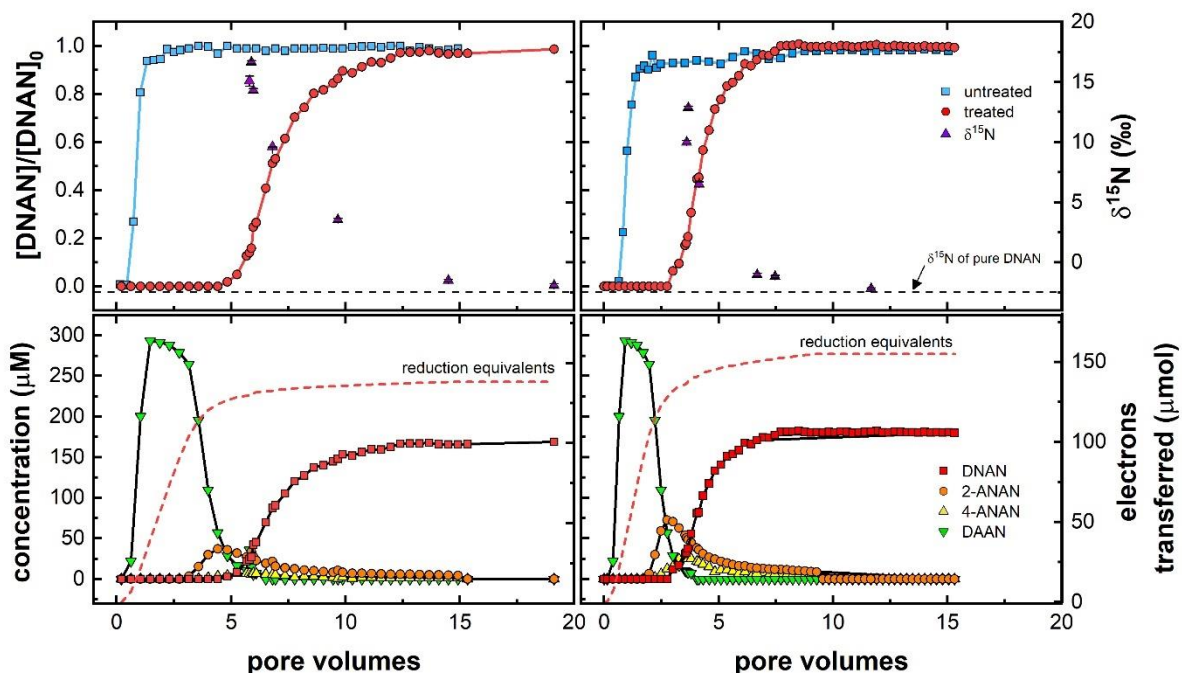


Figure 2. Breakthrough curves for 200 μM DNAN in (a) TCAAP and (b) Tinker AFB packed columns before (squares) and after (circles) receiving ISCR. Triangles denote measurements of $\delta^{15}\text{N}$ of DNAN in the column effluent. Error bars denote standard deviations from five sequential breakthrough experiments. Aqueous concentrations of DNAN (circles), 2-ANAN (squares), 4-ANAN (triangles), and DAAN (diamonds) during DNAN exposure to (c) TCAAP and (d) Tinker AFB columns. Dashed lines represent the cumulative number of reduction equivalents transferred to DNAN during experiments. The data provided in panels c and d are a representation of one of the reduction-reaction cycles shown in panels a and b, respectively. Individual cycles are shown in Figure S3.

the solution displaced DAAN from the surface. Such competition and effluent concentrations exceeding influents has been observed for ion sorption on activated carbon.⁸⁸ Another possible explanation is that a reaction intermediate (e.g., a hydroxylamine) is more strongly retained by the solid phase, as previously observed during the reduction of cyanonitrobenzene,⁸⁹ and the excess DAAN observed occurs once this intermediate has been reduced and released.

Despite ISCR targets that were equivalent to batch experiments (i.e., 10% reduction of Fe_T), the extent of electron transfer to DNAN from the reduced materials was markedly lower in columns than in batch experiments (0.143 ± 0.022 and 0.176 ± 0.020 mol e^-/mol Fe(II)) for TCAAP and

Tinker AFB columns, respectively; Table 1). This suggests that either (i) reactive Fe(II) was removed from the column, (ii) the transport of dithionite or DNAN to mineral surfaces was restricted by conditions within the column, or (iii) the extent of mineral reduction was affected by the rate of dithionite decomposition.

Flow-through systems introduce the potential for newly generated Fe(II) or other reducible species to be removed from the column before association with mineral surfaces or pollutant reduction occurs. Monitoring aqueous Fe(II) in column effluents, however, negligible losses of Fe(II) from the column were observed during and after exposure to dithionite (Figure S4). Only 1.6 and 5.3 μmol Fe(II) in TCAAP columns and 2.6 and 4.0 μmol Fe(II) in Tinker AFB columns were removed during the first and fifth exposures to dithionite, respectively, corresponding to 0.06–0.20% (w/w) of Fe_T . This suggests that Fe(II) generated during ISCR was mostly retained within the column either because it was not released from the mineral surfaces or it was effectively adsorbed by or bound within the materials within the column. The presence of silicates may also indicate a portion of Fe(II) that is not readily removed from natural soils and sediments. The consistency of breakthrough curves during the five cycles of ISCR and DNAN exposure (Figures S3) indicates that the removal of reduction equivalents by column flow likely did not affect the potential for contaminant reduction.

It is also possible that the transport of reducing equivalents or pollutants to mineral surfaces is restricted in confined systems composed of heterogenous media.⁹⁰ Moreover, the iron content of natural sediments can be distributed throughout the bulk mineral as opposed to being concentrated at singly-coordinated oxygen atoms on mineral surfaces, leaving Fe(III) inaccessible to dithionite. To account for these potential limitations, the columns in this study were packed to a uniform porosity (0.44 ± 0.05), bulk density ($1.66 \pm 0.04 \text{ g cm}^{-3}$), and particle density ($2.68 \pm 0.05 \text{ g cm}^{-3}$)

to resemble typical subsurface conditions in sandy soils similar to the TCAAP and Tinker AFB (Table S1).⁶⁸ The dispersion coefficients in TCAAP ($2.37 \pm 0.22 \text{ cm}^2 \text{ s}^{-1}$) and Tinker AFB ($2.53 \pm 12 \text{ cm}^2 \text{ s}^{-1}$) columns were also determined and indicated advection dominated regimes with negligible effects from flow retardation.⁹¹ Column porosities and dispersion coefficients were remeasured following all experiments and were not appreciably different from the initial values (Table S1), indicating that ISCR did not affect the physical properties of columns or restrict material transport.

Lastly, the rate of dithionite decomposition can unevenly distribute its reaction with iron in columns. In batch reactors, the entire supply of dithionite was simultaneously exposed to all of the solid material in a well-mixed heterogenous suspension, whereas, in columns only the materials located immediately following the inlet were exposed to unreacted dithionite. Because dithionite undergoes rapid disproportionation in aqueous media, the combination of Fe(III) reduction and dithionite decomposition limits mineral reduction at locations away from the point of application.^{11,48} These differences explain the difference between the batch and column experiments and provide an explanation for the lower extent of DNAN reduction in the column.

¹⁵N fractionation during DNAN reduction. DNAN reduction in batch reactors introduced strong ¹⁵N enrichment in the remaining contaminant with minor variations in magnitude (Figure 3). ¹⁵N isotope enrichment factors, ϵ_N , ranged from $-10.5 \pm 0.7\%$ to $-21.5 \pm 1.0\%$ in response to ¹⁵N-AKIEs of 1.021 ± 0.002 to 1.045 ± 0.001 . Because no C atoms are involved during the elementary steps of nitro-group reduction, C isotope fractionation was small and resulted in secondary ¹³C-AKIE values near unity (1.0005 ± 0.0003). These results are typical for nitro-group reduction on NACs by Fe(II) species associated with minerals (¹⁵N-AKIE = 1.030–1.045).^{43–45,73}

Our previous report of DNAN reduction by iron (oxyhydr)oxides revealed ϵ_N values between $-9 \pm 2\text{‰}$ and $-19 \pm 1\text{‰}$ corresponding to ^{15}N -AKIEs of 1.018 ± 0.002 and 1.039 ± 0.001 , respectively. The agreement in AKIEs between this and other reports of abiotic NAC reduction^{43–45} suggests that DNAN reduction followed the same reaction mechanism (i.e., nitro-group reduction) in the presence of Fe(II)-amended synthetic and natural materials and with the naturally collected materials after ISCR. Dual-element isotope analysis ($\delta^{15}\text{N}$ vs $\delta^{13}\text{C}$) was used to support this interpretation by illustrating the distinction of our results from other known DNAN transformation pathways (Figure S5).⁵⁷ For example, the correlation slope ($\Lambda^{N/C}$) calculated from this study was 43.8 ± 28.6 which is in clear contrast with independent evidence from biodegradation ($\Lambda^{N/C} = 0.87 \pm 0.15$) and alkaline hydrolysis ($\Lambda^{N/C} = 0.46 \pm 0.04$) experiments.⁵⁷ We previously reported a similar $\Lambda^{N/C}$ of 50.5 ± 23.2 during Fe(II)-mediated DNAN reduction by synthetic iron (oxyhydr)oxides.⁴⁰

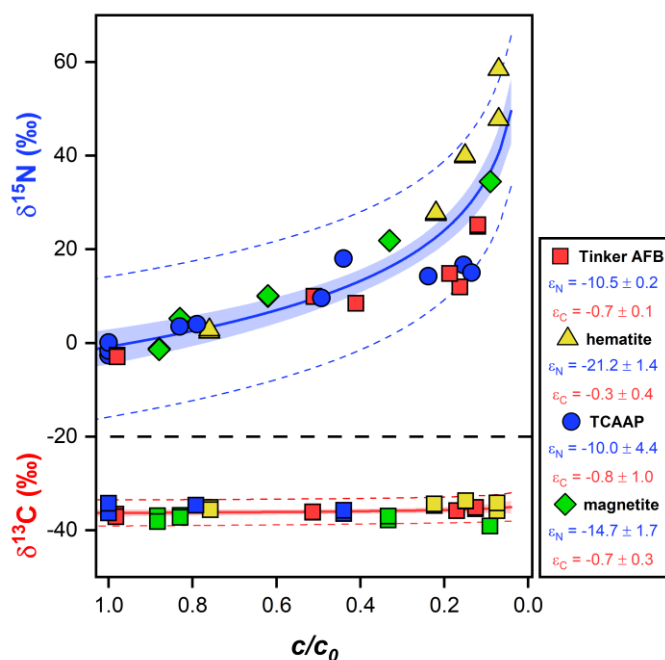


Figure 3. Nitrogen ($\delta^{15}\text{N}$) and carbon ($\delta^{13}\text{C}$) isotope signatures vs fraction of remaining substrate (c/c_0) during DNAN reduction by iron-bearing minerals. Solid lines represent fits from nonlinear

regression with shaded portions indicating the 95% confidence intervals. Dashed lines designate 95% prediction intervals. N and C isotope enrichment factors (ϵ_N , ϵ_C) were determined from non-linear regression of the data points for each mineral type. Data are shown for untreated materials in the presence of Fe(II) and dithionite-treated materials.

Quantifying DNAN transformation from ^{15}N enrichment in the residual contaminant. As shown in Figures 2a-b, $\delta^{15}\text{N}$ values of DNAN at the breakthrough front (~ 5 pore volumes) were isotopically enriched in ^{15}N corresponding to an increase of $\delta^{15}\text{N}$ by 15–20‰. Measured values subsequently decreased and approached the value for unreacted DNAN ($-2.4 \pm 0.1\text{‰}$) as the effluent concentrations approached the input level. This trend of $\delta^{15}\text{N}$ is consistent with the elution of an increasing share of DNAN that has not been reduced by surface-associated Fe(II). While the data provide evidence that ISCR promoted DNAN reduction, it should be noted that $\delta^{15}\text{N}$ values were not fully restored to the input $\delta^{15}\text{N}$ value suggesting the retention and slow release of enough residual ^{15}N -enriched DNAN from the mineral surfaces to influence the $\delta^{15}\text{N}$ after the reaction capacity was exhausted.^{92–94}

Taken together, all of our current data⁴⁰ for isotope fractionation during Fe(II)-catalyzed DNAN reduction in batch experiments resulted in a combined ϵ_N^* value of $-14.9 \pm 1.3\text{‰}$ (Figure S6a). This value was used to establish a relationship of c/c_0 vs $\Delta^{15}\text{N}$ (Figure S6b) to estimate the amount of DNAN degradation from $\delta^{15}\text{N}$ measurements made during column experiments (Figure 2a-b). Values of ϵ_N calculated from TCAAP ($-8.6 \pm 1.8\text{‰}$) and Tinker AFB ($-7.2 \pm 0.8\text{‰}$) column experiments were lower than batch experiments which could indicate longitudinal mixing with unreacted DNAN in the feed solution. A linear regression of predicted versus measured quantities was used to evaluate the accuracy of our estimates and showed a strong correlation (slope = 1.268 ± 0.176 , $r^2 = 0.958$) with a mean absolute error (MAE) of 0.091 ± 0.063 in c/c_0 indicating reasonable accuracy in the estimated values (Figure 4).

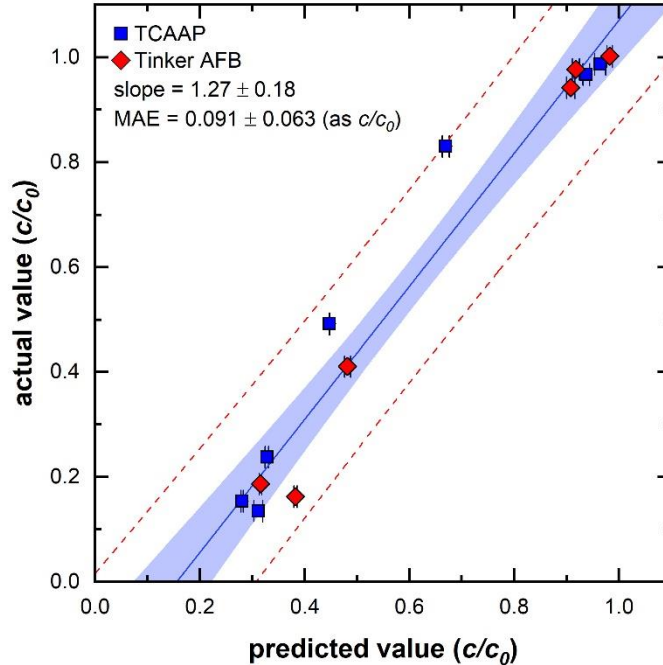


Figure 4. Predicted versus measured values of DNAN transformation by chemically reduced TCAAP and Tinker AFB materials in column reactors. Predictions were made according to eq 2 using an ϵ_N^* value of -14.9 ‰. Shaded portions indicate 95% confidence intervals of linear regressions and dashed lines represent the 95% prediction intervals.

The linearity of the regression in Figure 4 and the low MAE highlight the consistency between batch and column systems and underscore the ability for applying N isotope fractionation behavior of DNAN from laboratory data as reliable proxies of pollutant transformation in the field. Despite the specificity of our model to N isotopes, we also measured the accompanying $\delta^{13}\text{C}$ values to the $\delta^{15}\text{N}$ data shown in Figure 2a-b and observed minimal C isotope fractionation of DNAN at the breakthrough front ($\Delta^{13}\text{C} < \sim 3\text{‰}$; data in Figure S7). Because this C isotope fractionation was not observable after 6-7 pore volumes where N isotope fractionation continued, we consider it unlikely that another reaction such as concurrent (bio)degradation processes contributed to our observations. The distribution of $\delta^{13}\text{C}$ against $\delta^{15}\text{N}$ from column experiments also reflected the

batch systems (Figures 3 and S6) and supports that, in both cases, abiotic reduction was the primary reactive pathway.

Our study represents laboratory conditions and future work should continue to address direct applications of CSIA to contaminated field sites receiving ISCR. These analyses are also likely to underestimate the extent of DNAN degradation because contaminant flow through heterogeneous aquifers is directed along one of many flow paths which each introduce a unique extent and rate of (bio)degradation.²⁷ The flow paths that degrade the pollutant more quickly promote higher levels of fractionation; thus, downgradient contributions to the contaminant pool favor the unreacted (i.e., non-enriched) compound. To this end, the measured isotope ratios appear closer in magnitude to the source and may lead to low estimates of remediation. An understanding of the local hydrogeology is therefore necessary to accurately estimate the extent of contaminant (bio)degradation with CSIA.

Environmental significance. As remediation strategies are implemented, the adaptation of CSIA for pollutant monitoring in treated soil, sediment, and groundwater is critical for its successful integration into protocols for monitored natural attenuation and active remediation. To an extent, this has been accomplished but is limited to biodegradation²⁸ and synthetic minerals.⁴⁴ In this work, we reported CSIA as a robust technique to quantify abiotic DNAN reduction in systems receiving repeated dithionite treatments, but future work should include a survey of other *in situ* abiotic remediation strategies (e.g., calcium polysulfides,¹³ sodium persulfate⁹⁵). The observation that isotope fractionation is unaffected by natural subsurface materials and ISCR can be leveraged to generate accurate estimates of contaminant removal strengthen our findings. Moreover, it provides strong support for the compulsory lines of evidence set by the US

Environmental Protection Agency for evaluating the progress of natural attenuation.²⁷ Considering DNAN as a surrogate for other NACs allows for this approach to be applied to a wide range of environmental pollutants.

ACKNOWLEDGEMENTS

This work was supported by the Strategic Environmental Research and Development Program (SERDP, Project No. ER2618). Thanks to Lee Penn (UMN, Department of Chemistry) for allowing use of the X-ray diffractometer and to Jeanette L. Voelz (UMN, Department of Chemistry) for providing the hematite nanoparticles used in this study. ICP-OES analyses were performed by Clare Johnston (UMN, Department of Chemistry).

ASSOCIATED CONTENT

Supporting Information

A detailed report of additional analytical methods, materials synthesis and characterization techniques, batch reaction procedures, CSIA calculations, and further kinetics and isotope results.

The authors declare no competing interests.

REFERENCES

- (1) Ferrey, M. L.; Wilkin, R. T.; Ford, R. G.; Wilson, J. T. Nonbiological Removal of Cis-Dichloroethylene and 1,1-Dichloroethylene in Aquifer Sediment Containing Magnetite. *Environ. Sci. Technol.* **2004**, *38* (6), 1746–1752.

- (2) Hofstetter, T. B.; Heijman, C. G.; Haderlein, S. B.; Holliger, C.; Schwarzenbach, R. P. Complete Reduction of TNT and Other (Poly)Nitroaromatic Compounds under Iron-Reducing Subsurface Conditions. *Environ. Sci. Technol.* **1999**, *33* (9), 1479–1487.
- (3) Hofstetter, T. B.; Neumann, A.; Schwarzenbach, R. P. Reduction of Nitroaromatic Compounds by Fe (II) Species Associated with Iron-Rich Smectites. *Environ. Sci. Technol.* **2006**, *40* (1), 235–242.
- (4) Hofstetter, T. B.; Schwarzenbach, R. P.; Haderlein, S. B. Reactivity of Fe(II) Species Associated with Clay Minerals. *Environ. Sci. Technol.* **2003**, *37* (3), 519–528.
- (5) Butler, E. C.; Hayes, K. F. Effects of Solution Composition and PH on the Reductive Dechlorination of Hexachloroethane by Iron Sulfide. *Environ. Sci. Technol.* **1998**, *32*, 1276–1284.
- (6) Schaefer, C. E.; Ho, P.; Berns, E.; Werth, C. Mechanisms for Abiotic Dechlorination of Trichloroethene by Ferrous Minerals under Oxic and Anoxic Conditions in Natural Sediments. *Environ. Sci. Technol.* **2018**, *52* (23), 13747–13755.
- (7) Simpanen, S.; Dahl, M.; Gerlach, M.; Mikkonen, A.; Malk, V.; Mikola, J.; Romantschuk, M. Biostimulation Proved to Be the Most Efficient Method in the Comparison of in Situ Soil Remediation Treatments after a Simulated Oil Spill Accident. *Environ. Sci. Pollut. Res.* **2016**, *23* (24), 25024–25038.
- (8) McGuire, T. M.; Adamson, D. T.; Burcham, M. S.; Bedient, P. B.; Newell, C. J. Evaluation of Long-Term Performance and Sustained Treatment at Enhanced Anaerobic Bioremediation Sites. *Groundw. Monit. Remediat.* **2016**, *36* (2), 32–44.

- (9) Wu, Y.-J.; Liu, P.-W. G.; Hsu, Y.-S.; Whang, L.-M.; Lin, T.-F.; Hung, W.-N.; Cho, K.-C. Application of Molecular Biological Tools for Monitoring Efficiency of Trichloroethylene Remediation. *Chemosphere* **2019**, *233*, 697–704.
- (10) Schaefer, C. E.; Lavorgna, G. M.; Haluska, A. A.; Annable, M. D. Long-Term Impacts on Groundwater and Reductive Dechlorination Following Bioremediation in a Highly Characterized Trichloroethene DNAPL Source Area. *Groundw. Monit. Remediat.* **2018**, *38* (3), 65–74.
- (11) Amonette, J. E.; Szecsody, J. E.; Schaef, H. T.; Templeton, J. C.; Gorby, Y. A.; Fruchter, J. S. *Abiotic Reduction of Aquifer Materials by Dithionite: A Promising in-Situ Remediation Technology*; Richland, WA, USA, 1994.
- (12) Fruchter, J. S. J. S.; Cole, C. R. C. R.; Williams, M. D. M. D.; Vermeul, V. R.; Amonette, J. E. J. E.; Szecsody, J. E.; Istok, J. D.; Humphrey, M. D. Creation of a Subsurface Permeable Treatment Zone for Aqueous Chromate Contamination Using In Situ Redox Manipulation. *Groundw. Monit. Remediat.* **2000**, *20* (2), 66–77.
- (13) Graham, M. C.; Farmer, J. G.; Anderson, P.; Paterson, E.; Hillier, S.; Lumsdon, D. G.; Bewley, R. J. F. Calcium Polysulfide Remediation of Hexavalent Chromium Contamination from Chromite Ore Processing Residue. *Sci. Total Environ.* **2006**, *364* (1–3), 32–44.
- (14) Fan, D.; O'Brien Johnson, G.; G. Tratnyek, P.; L. Johnson, R. Sulfidation of Nano Zerovalent Iron (NZVI) for Improved Selectivity During In-Situ Chemical Reduction (ISCR). *Environ. Sci. Technol.* **2016**, *50* (17), 9558–9565.
- (15) Han, Y.; Yan, W. Reductive Dechlorination of Trichloroethene by Zero-Valent Iron

- Nanoparticles: Reactivity Enhancement through Sulfidation Treatment. *Environ. Sci. Technol.* **2016**, *50* (23), 12992–13001.
- (16) Niedźwiecka, J. B.; Finneran, K. T. Combined Biological and Abiotic Reactions with Iron and Fe(III)-Reducing Microorganisms for Remediation of Explosives and Insensitive Munitions (IM). *Environ. Sci. Water Res. Technol* **2015**, *1*, 34–39.
- (17) D. Ludwig, R.; Su, C.; R. Lee, T.; T. Wilkin, R.; D. Acree, S.; R. Ross, R.; Keeley, A. In Situ Chemical Reduction of Cr(VI) in Groundwater Using a Combination of Ferrous Sulfate and Sodium Dithionite: A Field Investigation. *Environ. Sci. Technol.* **2007**, *41* (15), 5299–5305.
- (18) Dresel, P. E.; Wellman, D. M.; Cantrell, K. J.; Truex, M. T. Review: Technical and Policy Challenges in Deep Vadose Zone Remediation of Metals and Radionuclides. *Environ. Sci. Technol.* **2011**, *45* (10), 4207–4216.
- (19) Szecsody, J. E.; Fruchter, J. S.; Williams, M. D.; Vermeul, V. R.; Sklarew, D. In Situ Chemical Reduction of Aquifer Sediments: Enhancement of Reactive Iron Phases and TCE Dechlorination. *Environ. Sci. Technol.* **2004**, *38* (17), 4656–4663.
- (20) Bonmatin, J. M.; Giorio, C.; Girolami, V.; Goulson, D.; Kreutzweiser, D. P.; Krupke, C.; Liess, M.; Long, E.; Marzaro, M.; Mitchell, E. A.; et al. Environmental Fate and Exposure; Neonicotinoids and Fipronil. *Environ. Sci. Pollut. Res.* **2015**, *22*, 35–67.
- (21) McKelvie, J. R.; Mackay, D. M.; de Sieyes, N. R.; Lacrampe-Couloume, G.; Sherwood Lollar, B. Quantifying MTBE Biodegradation in the Vandenberg Air Force Base Ethanol Release Study Using Stable Carbon Isotopes. *J. Contam. Hydrol.* **2007**, *94* (3–4), 157–165.

- (22) Chartrand, M.; Passeport, E.; Rose, C.; Lacrampe-Couloume, G.; Bidleman, T. F.; Jantunen, L. M.; Sherwood Lollar, B. Compound Specific Isotope Analysis of Hexachlorocyclohexane Isomers: A Method for Source Fingerprinting and Field Investigation of in Situ Biodegradation. *Rapid Commun. Mass Spectrom.* **2015**, *29* (6), 505–514.
- (23) Bosma, T. N. P.; Middeldorp, P. J. M.; Schraa, G.; Zehnder, A. J. B. Mass Transfer Limitation of Biotransformation: Quantifying Bioavailability. *Environ. Sci. Technol.* **1997**, *31* (1), 248–252.
- (24) Torrent, J.; Schwertmann, U.; Barron, V. The Reductive Dissolution of Synthetic Goethite and Hematite in Dithionite. *Clay Miner.* **1987**, *22* (3), 329–337.
- (25) Yang, L.; I. Steefel, C.; A. Marcus, M.; R. Bargar, J. Kinetics of Fe(II)-Catalyzed Transformation of 6-Line Ferrihydrite under Anaerobic Flow Conditions. *Environ. Sci. Technol.* **2010**, *44* (14), 5469–5475.
- (26) Amstaetter, K.; Borch, T.; Larese-Casanova, P.; Kappler, A. Redox Transformation of Arsenic by Fe(II)-Activated Goethite (α -FeOOH). *Environ. Sci. Technol.* **2009**, *44* (1), 102–108.
- (27) Hunkeler, D.; Meckenstock, R. U.; Lollar, B. S.; Schmidt, T. C.; Wilson, J. T. *A Guide for Assessing Biodegradation and Source Identification of Organic Ground Water Contaminants Using Compound Specific Isotope Analysis (CSIA)*; Oklahoma, USA, 2008.
- (28) Wijker, R. S.; Bolotin, J.; Nishino, S. F.; Spain, J. C.; Hofstetter, T. B. Using Compound-Specific Isotope Analysis to Assess Biodegradation of Nitroaromatic Explosives in the

- Subsurface. *Environ. Sci. Technol.* **2013**, *47* (13), 6872–6883.
- (29) Meckenstock, R. U.; Morasch, B.; Griebler, C.; Richnow, H. H. Stable Isotope Fractionation Analysis as a Tool to Monitor Biodegradation in Contaminated Aquifers. *J. Contam. Hydrol.* **2004**, *75* (3–4), 215–255.
- (30) Sherwood Lollar, B.; F. Slater, G.; Sleep, B.; Witt, M.; M. Klecka, G.; Harkness, M.; Spivack, J. Stable Carbon Isotope Evidence for Intrinsic Bioremediation of Tetrachloroethene and Trichloroethene at Area 6, Dover Air Force Base. *Environ. Sci. & Technol.* **2000**, *35* (2), 261–269.
- (31) Thullner, M.; Richnow, H. H.; Fischer, A. Characterization and Quantification of in Situ Biodegradation of Groundwater Contaminants Using Stable Isotope Fractionation Analysis: Advantages and Limitations. In *Environmental and Regional Air Pollution*; Nova Science Publishers, 2009.
- (32) Alvarez-Zaldívar, P.; Centler, F.; Maier, U.; Thullner, M.; Imfeld, G. Biogeochemical Modelling of in Situ Biodegradation and Stable Isotope Fractionation of Intermediate Chloroethenes in a Horizontal Subsurface Flow Wetland. *Ecol. Eng.* **2016**, *90*, 170–179.
- (33) Elsner, M.; Zwank, L.; Hunkeler, D.; Schwarzenbach, R. P. A New Concept Linking Observable Stable Isotope Fractionation to Transformation Pathways of Organic Pollutants. *Environ. Sci. Technol.* **2005**, *39* (18), 6896–6916.
- (34) Schmidt, T. C.; Zwank, L.; Elsner, M.; Berg, M.; Meckenstock, R. U.; Haderlein, S. B. Compound-Specific Stable Isotope Analysis of Organic Contaminants in Natural Environments: A Critical Review of the State of the Art, Prospects, and Future Challenges.

- Anal. Bioanal. Chem.* **2004**, 378 (2), 283–300.
- (35) Wijker, R. S.; Zeyer, J.; Hofstetter, T. B. Isotope Fractionation Associated with the Simultaneous Biodegradation of Multiple Nitrophenol Isomers by *Pseudomonas Putida* B2. *Environ. Sci. Process. Impacts* **2017**, 19 (5), 775–784.
- (36) Sherwood Lollar, B.; Slater, G.; Ahad, J.; Sleep, B.; Spivack, J.; Brennan, M.; MacKenzie, P. Contrasting Carbon Isotope Fractionation during Biodegradation of Trichloroethylene and Toluene: Implications for Intrinsic Bioremediation. *Org. Geochem.* **1999**, 30, 813–820.
- (37) Aeppli, C.; B. Hofstetter, T.; I. F. Amaral, H.; Kipfer, R.; P. Schwarzenbach, R.; Berg, M. Quantifying In Situ Transformation Rates of Chlorinated Ethenes by Combining Compound-Specific Stable Isotope Analysis, Groundwater Dating, And Carbon Isotope Mass Balances. *Environ. Sci. & Technol.* **2010**, 44 (10), 3705–3711.
- (38) Dodard, S. G.; Sarrazin, M.; Hawari, J.; Paquet, L.; Ampleman, G.; Thiboutot, S.; Sunahara, G. I. Ecotoxicological Assessment of a High Energetic and Insensitive Munitions Compound: 2,4-Dinitroanisole (DNAN). *J. Hazard. Mater.* **2013**, 262, 143–150.
- (39) Johnson, M. S.; Eck, W. S.; Lent, E. M. Toxicity of Insensitive Munition (IMX) Formulations and Components. *Propellants, Explos. Pyrotech.* **2017**, 42 (1), 9–16.
- (40) Berens, M. J.; Ulrich, B. A.; Strehlau, J. H.; Hofstetter, T. B.; Arnold, W. A. Mineral Identity, Natural Organic Matter, and Repeated Contaminant Exposures Do Not Affect the Carbon and Nitrogen Isotope Fractionation of 2,4-Dinitroanisole during Abiotic Reduction. *Environ. Sci. Process. Impacts* **2019**, 21, 51–62.
- (41) Boparai, H. K.; Comfort, S. D.; Shea, P. J.; Szecsody, J. E. Remediating Explosive-

- Contaminated Groundwater by in Situ Redox Manipulation (ISRM) of Aquifer Sediments. *Chemosphere* **2008**, 71 (5), 933–941.
- (42) He, F.; Zhao, D.; Paul, C. Field Assessment of Carboxymethyl Cellulose Stabilized Iron Nanoparticles for in Situ Destruction of Chlorinated Solvents in Source Zones. *Water Res.* **2010**, 44 (7), 2360–2370.
- (43) Hofstetter, T. B.; Neumann, A.; Arnold, W. A.; Hartenbach, A. E.; Bolotin, J.; Cramer, C. J.; Schwarzenbach, R. P. Substituent Effects on Nitrogen Isotope Fractionation during Abiotic Reduction of Nitroaromatic Compounds. *Environ. Sci. Technol.* **2008**, 42 (6), 1997–2003.
- (44) Hartenbach, A.; Hofstetter, T. B.; Berg, M.; Bolotin, J.; Schwarzenbach, R. P. Using Nitrogen Isotope Fractionation to Assess Abiotic Reduction of Nitroaromatic Compounds. *Environ. Sci. Technol.* **2006**, 40 (24), 7710–7716.
- (45) Hartenbach, A. E.; Hofstetter, T. B.; Aeschbacher, M.; Sander, M.; Kim, D.; Strathmann, T. J.; Arnold, W. A.; Cramer, C. J.; Schwarzenbach, R. P. Variability of Nitrogen Isotope Fractionation during the Reduction of Nitroaromatic Compounds with Dissolved Reductants. *Environ. Sci. Technol.* **2008**, 42 (22), 8352–8359.
- (46) Pichtel, J. Distribution and Fate of Military Explosives and Propellants in Soil: A Review. *Appl. Environ. Soil Sci.* **2012**, 2012 (2012).
- (47) Albright, R. D. *Cleanup of Chemical and Explosive Munitions - Locating, Identifying Contaminants, and Planning for Environmental Remediation of Land and Sea Military Ranges and Ordnance Dumpsites*, 2nd ed.; William Andrew: Norwich, NY, USA, 2012.

- (48) Istok, J. D.; Amonette, J. E.; Cole, C. R.; Fruchter, J. S.; Humphrey, M. D.; Szecsody, J. E.; Teel, S. S.; Vermeul, V. R.; Williams, M. D.; Yabusaki, S. B. In Situ Redox Manipulation by Dithionite Injection: Intermediate-Scale Laboratory Experiments. *Ground Water* **1999**, *37*, 884–889.
- (49) Hocking, G.; Givens, M. A.; Thurman, C. M.; Lacko, C. M. Installation of Permeable Reactive Barrier at Tinker Air Force Base, Oklahoma City, Oklahoma. In *5th International Conference on Remediation of Chlorinated and Recalcitrant Compounds*; Monterey, CA, 2006.
- (50) Voelz, J.; Arnold, W. A.; Penn, R. L. Redox-Induced Nucleation and Growth of Goethite on Synthetic Hematite Nanoparticles. *Am. Mineral.* **2018**, *103*, 1021–1029.
- (51) Strehlau, J. H.; Berens, M. J.; Arnold, W. A. Mineralogy and Buffer Identity Effects on RDX Kinetics and Intermediates during Reaction with Natural and Synthetic Magnetite. *Chemosphere* **2018**, *213*, 602–609.
- (52) Cornell, R. M.; Giovanoli, R. Acid Dissolution of Hematites of Different Morphologies. *Clay Miner.* **1993**, *28* (2), 223–232.
- (53) Cornell, R. M.; Giovanoli, R. Acid Dissolution of Akaganeite and Lepidocrocite: The Effect on Crystal Morphology. *Clays Clay Miner.* **1988**, *36* (5), 385–390.
- (54) Viollier, E.; Inglett, P. W.; Hunter, K.; Roychoudhury, A. N.; Van Cappellen, P. The Ferrozine Method Revisited: Fe(II)/Fe(III) Determination in Natural Waters. *Appl. Geochemistry* **2000**, *15* (6), 785–790.
- (55) Sumner, M. E.; Miller, W. P. Cation Exchange Capacity and Exchange Coefficients. In

Methods of Soil Analysis Part 3 - Chemical Methods; 1996; pp 1201–1229.

- (56) Berg, M.; Bolotin, J.; Hofstetter, T. B. Compound-Specific Nitrogen and Carbon Isotope Analysis of Nitroaromatic Compounds in Aqueous Samples Using Solid-Phase Microextraction Coupled to GC/IRMS. *Anal. Chem.* **2007**, *79* (6), 2386–2393.
- (57) Ulrich, B. A.; Palatucci, M.; Bolotin, J.; Spain, J. C.; Hofstetter, T. B. Different Mechanisms of Alkaline and Enzymatic Hydrolysis of the Insensitive Munition Component 2,4-Dinitroanisole Lead to Identical Products. *Environ. Sci. Technol. Lett.* **2018**, *5* (7), 456–461.
- (58) Kremser, A.; Jochmann, M. A.; Schmidt, T. C. PAL SPME Arrow - Evaluation of a Novel Solid-Phase Microextraction Device for Freely Dissolved PAHs in Water. *Anal. Bioanal. Chem.* **2016**, *408* (3), 943–952.
- (59) Pati, S. G.; Kohler, H.-P. E.; Hofstetter, T. B. Characterization of Substrate, Cosubstrate, and Product Isotope Effects Associated with Enzymatic Oxygenations of Organic Compounds Based on Compound-Specific Isotope Analysis. In *Methods in Enzymology*; Elsevier Inc., 2017; Vol. 596, pp 291–329.
- (60) Schimmelmann, A.; Albertino, A.; Sauer, P. E.; Qi, H.; Molinie, R.; Mesnard, F. Nicotine, Acetanilide and Urea Multi-Level 2H -, 13C - and 15N -Abundance Reference Materials for Continuous-Flow Isotope Ratio Mass Spectrometry. *Rapid Commun. Mass Spectrom.* **2009**, *23* (22), 3513–3521.
- (61) Elsner, M. Stable Isotope Fractionation to Investigate Natural Transformation Mechanisms of Organic Contaminants: Principles, Prospects and Limitations. *J. Environ. Monit.* **2010**, *12* (11), 2005–2031.

- (62) G. B. Williams, A.; M. Scherer, M. Spectroscopic Evidence for Fe(II)–Fe(III) Electron Transfer at the Iron Oxide–Water Interface. *Environ. Sci. Technol.* **2004**, *38* (18), 4782–4790.
- (63) Klausen, J. J.; Tröber, S. P.; Haderlein, S. B.; Schwarzenbach, R. P.; Troeber, S. P.; Haderlein, S. B.; Schwarzenbach, R. P. Reduction of Substituted Nitrobenzenes by Fe(II) in Aqueous Mineral Suspensions. *Environ. Sci. Technol.* **1995**, *29* (9), 2396–2404.
- (64) Amonette, J. E.; Workman, D. J.; Kennedy, D. W.; Fruchter, J. S.; Gorby, Y. A. Dechlorination of Carbon Tetrachloride by Fe(II) Associated with Goethite. *Environ. Sci. Technol.* **2000**, *34* (21), 4606–4613.
- (65) Elsner, M.; Schwarzenbach, R. P.; Haderlein, S. B. Reactivity of Fe(II)-Bearing Minerals toward Reductive Transformation of Organic Contaminants. *Environ. Sci. Technol.* **2004**, *38* (3), 799–807.
- (66) Fan, D.; J. Bradley, M.; W. Hinkle, A.; L. Johnson, R.; G. Tratnyek, P. Chemical Reactivity Probes for Assessing Abiotic Natural Attenuation by Reducing Iron Minerals. *Environ. Sci. Technol.* **2016**, *50* (4), 1868–1876.
- (67) Voelz, J. L.; Johnson, N. W.; Chun, C. L.; Arnold, W. A.; Penn, R. L. Quantitative Dissolution of Environmentally Accessible Iron Residing in Iron-Rich Minerals: A Review. *ACS Earth Sp. Chem.* **2019**, *3* (8), 1371–1392.
- (68) Essington, M. E. *Soil and Water Chemistry: An Integrative Approach*, 2nd ed.; CRC Press, 2015.
- (69) Guo, H.; Barnard, A. S. Naturally Occurring Iron Oxide Nanoparticles: Morphology,

- Surface Chemistry and Environmental Stability. *J. Mater. Chem. A* **2013**, *1* (January 2013), 27–42.
- (70) Schwertmann, U.; Cornell, R. M. *Iron Oxides in the Laboratory: Preparation and Characterization*, 2nd ed.; Wiley-VCH: Weinheim, 2000.
- (71) Strehlau, J. H.; Toner, B. M.; Arnold, W. A.; Penn, R. L. Accessible Reactive Surface Area and Abiotic Redox Reactivity of Iron Oxyhydroxides in Acidic Brines. *Geochim. Cosmochim. Acta* **2017**, *197*, 345–355.
- (72) James, B. R.; Brose, D. A. Oxidation-Reduction Phenomena. In *Handbook of Soil Science: Properties and Processes*; CRC Press: Boca Raton, FL, 2012; pp 14-1-14–24.
- (73) Gorski, C. A.; Nurmi, J. T.; Tratnyek, P. G.; Hofstetter, T. B.; Scherer, M. M. Redox Behavior of Magnetite: Implications for Contaminant Reduction. *Environ. Sci. Technol.* **2010**, *44* (1), 55–60.
- (74) Gorski, C. A.; Scherer, M. M. Influence of Magnetite Stoichiometry on FeII Uptake and Nitrobenzene Reduction. *Environ. Sci. Technol.* **2009**, *43* (10), 3675–3680.
- (75) Haggstrom, L.; Annersten, H.; Ericsson, T.; Wappling, R.; Karner, W.; Bjarman, S. Magnetic Dipolar and Electric Quadrupolar Effects on the Mossbauer Spectra of Magnetite above the Verwey Transition. *Hyperfine Interact.* **1977**, *5* (1), 201–214.
- (76) Vandenberghe, R. E.; Hus, J. J.; De Grave, E. Evidence from Mössbauer Spectroscopy of Neo-Formation of Magnetite/Maghemite in the Soils of Loess/Paleosol Sequences in China. *Hyperfine Interact.* **1998**, *117* (1/4), 359–369.
- (77) Wehrli, B.; Sulzberger, B.; Stumm, W. Redox Processes Catalyzed by Hydrous Oxide

- Surfaces. *Chem. Geol.* **1989**, 78 (3–4), 167–179.
- (78) Torrent, J.; Barron, V. Iron Oxides in Relation to the Colour of Mediterranean Soils. In *Applied Study of Cultural Heritage and Clays*; 2003; pp 377–386.
- (79) Lovley, D. R.; Coates, J. D.; Blunt-Harris, E. L.; Phillips, E. J. P.; Woodward, J. C. Humic Substances as Electron Acceptors for Microbial Respiration. *Nature* **1996**, 382, 445–448.
- (80) Scott, D. T.; Mcknight, D. M.; Blunt-Harris, E. L.; Kolesar, S. E.; Lovley, D. R. Quinone Moieties Act as Electron Acceptors in the Reduction of Humic Substances by Humics-Reducing Microorganisms. *Environ. Sci. Technol.* **1998**, 32 (19), 2984–2989.
- (81) Lovley, D. R.; Fraga, J. L.; Coates, J. D.; Blunt-Harris, E. L. Humics as an Electron Donor for Anaerobic Respiration. *Environ. Microbiol.* **1999**, 1 (1), 89–98.
- (82) Ratasuk, N.; A. Nanny, M. Characterization and Quantification of Reversible Redox Sites in Humic Substances. *Environ. Sci. Technol.* **2007**, 41 (22), 7844–7850.
- (83) M. Dunnivant, F.; P. Schwarzenbach, R.; L. Macalady, D. Reduction of Substituted Nitrobenzenes in Aqueous Solutions Containing Natural Organic Matter. *Environ. Sci. Technol.* **1992**, 26 (11), 2133–2141.
- (84) Deiana, S.; Gessa, C.; Manunza, B.; Rausa, R.; Solinas, V. Iron(III) Reduction by Natural Humic Acids: A Potentiometric and Spectroscopic Study. *Eur. J. Soil Sci.* **1995**, 46 (1), 103–108.
- (85) Beyer, M. E.; Bond, A. M.; McLaughlin, R. J. W. Simultaneous Polarographic Determination of Ferrous, Ferric, and Total Iron in Standard Rocks. *Anal. Chem.* **2002**, 47 (3), 479–482.

- (86) Haese, R. R.; Wallmann, K.; Dahmke, A.; Kretzmann, U.; Müller, P. J.; Schulz, H. D. Iron Species Determination to Investigate Early Diagenetic Reactivity in Marine Sediments. *Geochim. Cosmochim. Acta* **1997**, *61* (1), 63–72.
- (87) Neumann, A.; Hofstetter, T. B.; Lüssi, M.; Cirpka, O. A.; Petit, S.; Schwarzenbach, R. P. Assessing the Redox Reactivity of Structural Iron in Smectites Using Nitroaromatic Compounds As Kinetic Probes. *Environ. Sci. Technol.* **2008**, *42* (22), 8381–8387.
- (88) Erickson, A. J.; Gulliver, J. S.; Arnold, W. A.; Brekke, C.; Bredal, M. Abiotic Capture of Stormwater Nitrates with Granular Activated Carbon. *Environ. Eng. Sci.* **2016**, *33* (5), 354–363.
- (89) Simon, R.; Colón, D.; L. Tebes-Stevens, C.; J. Weber, E. Effect of Redox Zonation on the Reductive Transformation of P-Cyanonitrobenzene in a Laboratory Sediment Column. *Environ. Sci. & Technol.* **2000**, *34* (17), 3617–3622.
- (90) Freeze, R. A.; Cherry, J. A. *Groundwater*, 1st ed.; Prentice Hall, 1979.
- (91) Gulliver, J. S. *Introduction to Chemical Transport in the Environment*; Cambridge University Press: Cambridge, 2007.
- (92) B. Haderlein, S.; W. Weissmahr, K.; P. Schwarzenbach, R. Specific Adsorption of Nitroaromatic Explosives and Pesticides to Clay Minerals. *Environ. Sci. & Technol.* **1996**, *30* (2), 612–622.
- (93) Arthur, J. D.; Mark, N. W.; Taylor, S.; Šimunek, J.; Brusseau, M. L.; Dontsova, K. M. Batch Soil Adsorption and Column Transport Studies of 2,4-Dinitroanisole (DNAN) in Soils. *J. Contam. Hydrol.* **2017**, *199*, 14–23.

- (94) B. Haderlein, S.; P. Schwarzenbach, R. Adsorption of Substituted Nitrobenzenes and Nitrophenols to Mineral Surfaces. *Environ. Sci. Technol.* **1993**, *27* (2), 316–326.
- (95) Tsitonaki, A.; Petri, B.; Crimi, M.; Mosbk, H.; Siegrist, R. L.; Bjerg, P. L. In Situ Chemical Oxidation of Contaminated Soil and Groundwater Using Persulfate: A Review. *Crit. Rev. Environ. Sci. Technol.* **2010**, *40* (1), 55–91.

TOC Art

